ACS OMEGA

Article

Cite This: ACS Omega 2018, 3, 12851−12856

http://pubs.acs.org/journal/acsodf

Transoid-to-Cisoid Conformation Changes of Single Molecules on Surfaces Triggered by Metal Coordination

Sara Freund,[†] Rémy Pawlak,*[,†] Lucas Moser,[†] Antoine Hinaut,[†] Roland Steiner,[†] Nathalie Marinakis,[‡] Edwin C. Constable,[‡] Ernst Meyer,[†] Catherine E. Housecroft,[‡] and Thilo Glatzel[†]

[†]Department of Physics, University of Basel, Klingelbergstrasse 82, CH-4056 Basel, Switzerland

[‡]Department of Chemistry, University of Basel, Mattenstrasse 24a, BPR 1096, CH-4058 Basel, Switzerland

ABSTRACT: Conformational isomers are stereoisomers that can interconvert over low potential barriers by rotation around a single bond. However, such bond rotation is hampered by geometrical constraints when molecules are adsorbed on surfaces. Here, we show that the adsorption of 4,4′-bis(4-carboxyphenyl)-6,6′-dimethyl-2,2′-bipyridine molecules on surfaces leads to the appearance of prochiral single molecules on NiO(001) and to enantiopure supramolecular domains on Au(111) surfaces containing the transoid-molecule conformation. Upon additional Fe adatom deposition, molecules undergo a controlled interconversion from a transoid-to-cisoid conformation as a result of coordination of the Fe atoms to the 2,2′-bipyridine moieties. As confirmed by atomic force microscopy images and X-ray photoelectron spectroscopy measurements, the resulting molecular structures become irreversibly achiral.

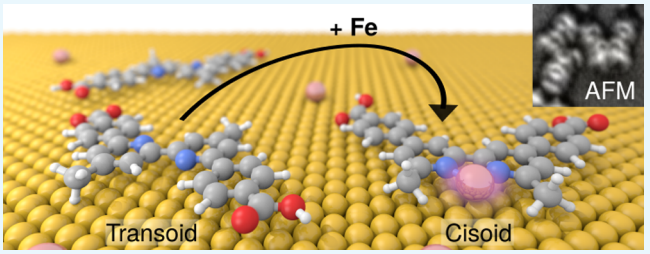

INTRODUCTION

An enantiomer is "one of a pair of molecular entities which are mirror images of each other and non-superposable".[1] Atropisomerism is a particular class of axial enantiomerism which results from hindered rotation about a single bond. In such compounds, enantiomer interconversions are mediated only by bond rotations between isomers (in contrast to interconversions that involve covalent bond breaking). Thus, the stability of "long-lived" atropisomers in three dimensions usually requires steric hindrance in order to constrain internal bond rotations using peripheral chemical substitutions. To impose chirality, another approach consists in the confinement of molecules onto a crystalline surface. Over the last couple of decades, this strategy has enabled the formation of enantiopure self-assemblies[2,3] or chiral molecular compounds from on-surface chemical reactions.[4,5] Accessing chiral molecular surfaces further allows a vast range of novel properties to emerge including the amplification of nonlinear optical properties[6,7] and the asymmetric scattering of spin-polarized electrons.[8] Moreover, the control of chiral−achiral transitions in surface-stabilized molecular networks could also help designing chirality sensors, molecular switches, and motors.[9−11] If a good alternative for stabilizing relies in their geometrical frustration on a surface,[12,13] a step further would be to control the bond rotation and thus the molecule conformation.

In this work, we investigate the adsorption of achiral 4,4′-di(4-carboxyphenyl)-6,6′-dimethyl-2,2′-bipyridine (DCPDMbpy) molecules by means of atomic force microscopy (AFM), scanning tunneling microscopy (STM), and X-ray photoelectron spectroscopy (XPS) on NiO(001) and Au(111). Our work is motivated by our recent hierarchical assembly strategy "surfaces-as-ligands surfaces-as-complexes" approach[14] focusing on designing novel molecular compounds having (i) anchoring groups such as carboxylic or phosphonic acids that enable a strong anchoring of the molecule to surfaces and (ii) metal-binding moieties such as 2,2′-bipyridine (bpy) to facilitate the assembly of surface-bound metal coordination compounds either through sequential addition of metal ions and an ancillary ligand or through a ligand−exchange reaction between the anchoring ligand and a homoleptic metal complex.[14−17]

In a previous work, we investigated the first step of the DCPDMbpy assembly process using AFM operated in ultrahigh vacuum (UHV) conditions.[18] We showed that the DCPDMbpy molecule systematically adopts two prochiral transoid conformations (α and β, Figure 1a) when adsorbed onto an atomically clean NiO(001) crystal surface. In contrast, the cisoid conformation was not observed even upon annealing up to 420 K close to the desorption temperature of the molecule. This can be explained by the high energy barrier needed to be overcome in order to induce a bond rotation about the interannular C−C bond as well as the energy to partially desorb the molecule from the surface to allow the rotation.

Theoretical studies of the conformational change from transoid to cisoid for a bpy in the gas phase have estimated an energy of about 320 meV (31 kJ·mol^{-1}).[19,20] The high

Received: July 27, 2018
Accepted: September 20, 2018
Published: October 9, 2018

DOI: 10.1021/acsomega.8b01792
ACS Omega 2018, 3, 12851−12856

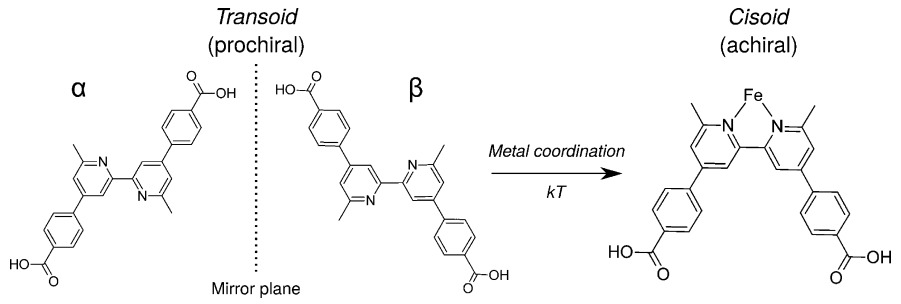

Figure 1. Transoid and cisoid conformations of the DCPDMbpy and Fe−DCPDMbpy molecules. Upon adsorption, the DCPDMbpy adopts two prochiral conformations α and β. Upon coordination with Fe, the molecule can undergo a conformational change to the cisoid conformation.

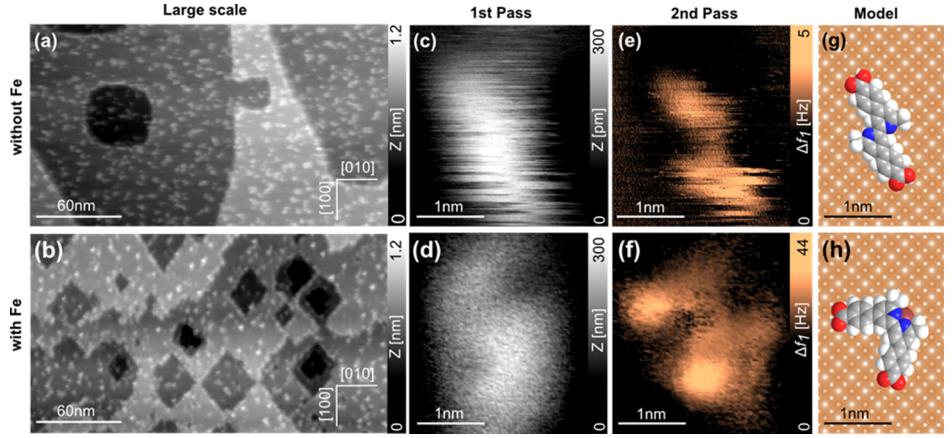

Figure 2. Transoid and cisoid conformations of DCPDMbpy molecules adsorbed on NiO(001). Large-scale AFM topographic images of NiO(001): (a) after deposition of DCPDMbpy molecules and (b) after deposition of Fe and DCPDMbpy molecules (scan parameters: A_1 = 4 nm, Δf_1 = −3 Hz and Δf_1 = −10 Hz, respectively). (c,d) AFM topographic images of flat-lying single molecules adsorbed before and after Fe deposition, respectively. The images were acquired using the first scanning pass (scan parameters: A_1 = 4 nm, Δf_1 = −2.5 Hz, and Δf_1 = 29 Hz, respectively). (e,f) Corresponding Δf images acquired with the second scanning pass, that is, with open feedback, using offsets of ∼−350 and −280 pm. The molecules are in transoid and cisoid conformation, respectively. (g,h) Structural models of both DCPDMbpy geometries on NiO(001).

rotational barrier was found to arise from the electrostatic repulsion between the lone pairs of the bipyridine units.[21] This repulsive interaction also leads to the transoid conformation in favor of the cisoid one in gas phase as well as during its adsorption on surfaces. Note that this barrier is much higher than the available thermal energy at room temperature (RT) or even upon surface annealing (i.e., at 1000 K, the available energy is about 80 meV (8 kJ·mol^{-1}), which implies that the molecule desorbs before changing its conformation to the cisoid one). However, the activation energy to promote the conformational change can be overcome when forming a complex between a metal atom and a bpy unit, theoretically delivering about 4.66 eV (450 kJ·mol^{-1}).[22,23] Metal coordination might thus enable the emergence of the cisoid form on surfaces.

Here, we investigated DCPDMbpy molecules in the presence of metallic adatoms on both NiO(001) and Au(111) surfaces. The achiral cisoid geometry is observed after adsorption of prochiral DCPDMbpy on a NiO(001) surface previously partially covered with Fe atoms, demonstrating the Fe−DCPDMbpy complex formation through coordination between Fe atoms and bpy moieties. Furthermore, upon Fe adatom deposition on prochiral DCPDMbpy assemblies formed on Au(111), the molecules undergo an interconversion from transoid to cisoid on the surface, which is triggered by the same metal-coordination mechanism as shown by AFM images and XPS measurements.

RESULTS AND DISCUSSION

Conformations of the DCPDMbpy and Fe−DCPDMbpy Molecules on NiO(001) at RT. To demonstrate the control of such chiral−achiral transitions on surfaces, we first investigated DCPDMbpy molecules on a NiO(001) substrate. Figure 2a shows a representative AFM topographic image of the NiO(001) surface after deposition of 0.2 monolayer (ML) of DCPDMbpy at RT. In the following, we define a ML as one layer of molecules fully covering the surface, 0.2 ML corresponds to a surface coverage of 20%. Large terraces are separated by mono-atomic steps and are covered with single molecules as well as molecular aggregates. The step edges are saturated on both upper and lower sides, indicating that these are preferential adsorption sites. The relatively short distance between the molecules (3.9 ± 0.7 nm in average) suggests a relatively low diffusion of the molecules at RT on the NiO(001) surface and, therefore, a rather strong binding to the substrate. Upon surface annealing, the diffusion remains low as discussed previously,[18] where molecular diffusion as a function of the substrate annealing temperature was studied.

In order to trigger the emergence of metal complexes, 0.1 ML of Fe atoms was deposited at RT on the bare surface of NiO. DCPDMbpy molecules were then subsequently adsorbed onto this surface. To favor the coordination complex formation, the sample was annealed to 420 K after sublimation of molecules. Figure 2b shows an AFM topographic image of

DOI: 10.1021/acsomega.8b01792
ACS Omega 2018, 3, 12851−12856

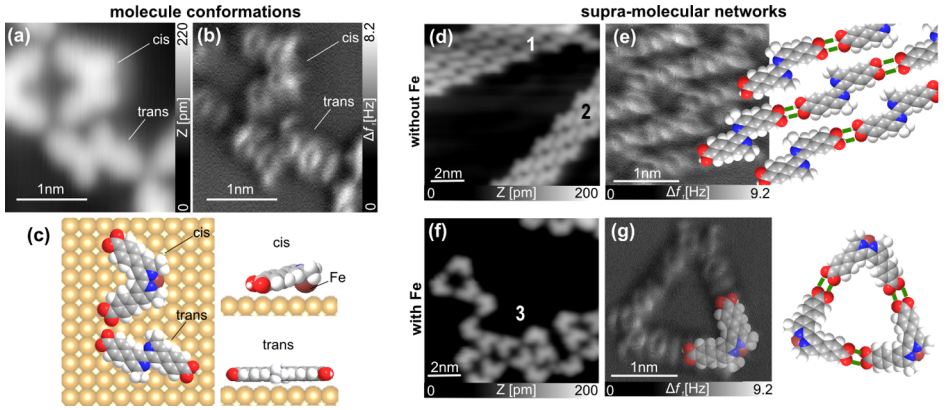

Figure 3. High-resolution imaging of the transoid and cisoid conformations of DCPDMbpy and Fe−DCPDMbpy with CO-terminated tips. (a) STM image of the molecules in transoid and cisoid conformation. (b) Corresponding AFM image of the two same molecules with intramolecular resolution. (c) Structural models of DCPDMbpy in transoid- and Fe−DCPDMbpy in cisoid conformations. (d) Self-assemblies of transoid-DCPDMbpy on Au(111) leading to two enantiopure domains denoted 1 and 2, respectively. (e) Tentative structural model of H-bonded enantiopure molecular domains 1 superimposed to an AFM image of the assembly with a CO-terminated tip. (f) STM image of the molecular network obtained by adding Fe atoms on Au(111). The prochirality of the molecule domain is lost because of the metal-complex formation. (g) Tentative structural model an AFM image of the H-bonded Fe−DCPDMbpy molecules in their cisoid conformation on Au(111). (Scan parameters: STM images: I_t = 1 pA, V = −0.15 V and AFM images: A = 50 pm, V = 0 V).

this surface. To unambiguously confirm the DCPDMbpy−Fe complex formation on NiO(001), we focused on imaging of the molecule conformations at RT using a silicon cantilever (see Methods), employing the multipass technique[24] which has proven to deliver submolecular resolution at RT.[18,25] The method consists of recording a first line scan with a closed feedback loop at a relative tip−sample distance Z_{1st} regulated for a particular set-point Δf_1 and acquiring a second pass along the same scan line with the feedback open and at a closer tip−sample distance $Z_{2nd} = Z_{1st} - Z_{off}$ (Z_{off} is in the order of 200−400 pm).

Figure 2c,d shows such AFM images of the DCPDMbpy molecules on NiO(001) without and with Fe atoms, respectively. The two AFM images acquired during the first scan suggest that both molecules are lying flat on the surface (∼0.2 nm in height) but the lack of resolution does not allow us to unambiguously assign a conformation. In the second pass, the molecules are better resolved (Figure 2e,f) and a clear distinction between the transoid and cisoid conformations of both molecules is observed as illustrated in Figure 2g,h. Upon adsorption and without Fe atoms, the DCPDMbpy molecules are adsorbed in the prochiral transoid conformation, whereas successive deposition of Fe and molecules results in the formation of the Fe−DCPDM(bpy) units possessing the cisoid conformation within the bpy units. Although the adoption of the cisoid conformation is due to the coordination to a metal center, we cannot clearly confirm its presence by AFM imaging. Metal atoms are generally difficult to observe by AFM in metal−ligand complexes at surfaces.[26−30]

Structure Resolution by Low-Temperature AFM with CO-Terminated Tips. To further improve the resolution, we measured the DCPDMbpy molecules on Au(111) at 4.7 K using AFM with a CO-terminated tip.[31] Compared to the NiO(001) samples, Au(111) surfaces were prepared with similar molecule and Fe atom coverages (see Methods). Figure 3a,b shows STM topographies of both DCPDMbpy conformations and the corresponding constant-height AFM image acquired with a CO-terminated tip at 4.7 K. The transoid and cisoid conformations are unambiguously observed, and a clear distinction of the phenyl rings of the molecules as well as the methyl groups attached to the bpy units again confirms that the molecules lie flat on the surface (see qualitative models in Figure 3c). For the cisoid conformation, the Fe atom bound to the bpy moieties is again not visible in the image. This observation, in addition to the fact that the methyl groups of the Fe−DCPDMbpy appear with a brighter contrast in comparison to transoid−DCPDMbpy, suggest that the Fe atom is hidden under the molecule with the result that the latter undergoes a slight bending (Figure 3c).

The diffusion of the DCPDMbpy on Au(111) in comparison to what is observed on NiO(001) plays an important role. Indeed, in contrast to NiO, large DCPDMbpy self-assemblies can be formed at the gold surface at RT even at low coverages (≤0.2 ML) as shown in Figure 3d. In other words, the diffusion of each product of the reaction and consequently also the formation of supramolecular structures can be hindered or facilitated as a function of the host substrate. On Au(111), two enantiopure domains denoted 1 and 2 coexist as a direct consequence of the prochirality of the DCPDMbpy molecule. As shown in the AFM image and highlighted by green lines in the structural model of Figure 3e, the self-assembly process is governed by hydrogen bonding between carboxylic groups of adjacent enantiomers and forms extended close-packed molecular domains. The additional deposition of Fe atoms onto these chiral molecular domains on Au(111) leads to the formation of extended chainlike structures (Figures 3f and 4d). By interacting with the lone pairs of the bipyridine unit, the Fe atom in the Fe−DCPDMbpy complex imposes the cisoid conformation. This conformation is achiral on the surface and, thus, induces the loss of chirality of the molecular domains.

In analogy to the self-assembly of transoid molecules, the assembly of cisoid Fe−DCPDMbpy complex is driven by hydrogen bonding between their carboxylic groups (O−H···O) leading to the formation of chainlike assemblies (Figures 3f and 4d) as well as trimers (Figure 3g). Note that the coordination of more than one DCPDMbpy ligand to Fe was never observed on the surface. We attribute this to the steric hindrance that would occur between the 6,6′-dimethyl groups

DOI: 10.1021/acsomega.8b01792
ACS Omega 2018, 3, 12851−12856

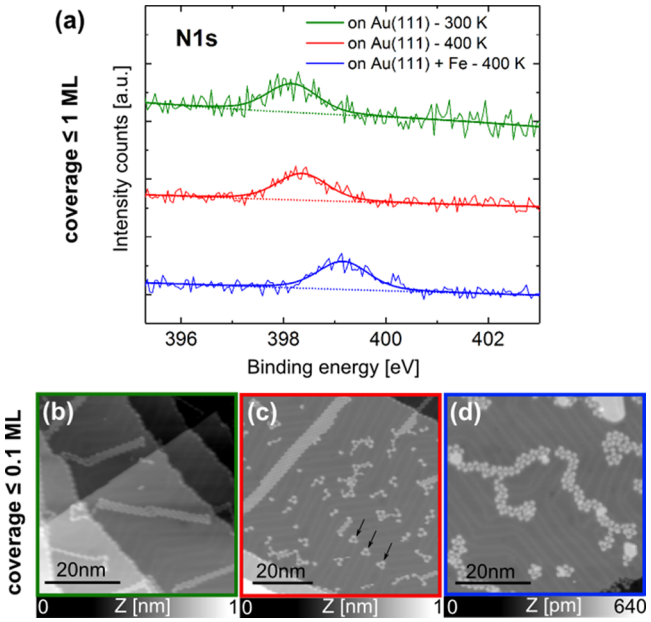

Figure 4. N 1s core level spectra. (a) XPS of one ML coverage of DCPDMbpy on Au(111) adsorbed at RT (green), after annealing at 400 K (red) and after annealing at 400 K and Fe deposition (blue). The shown spectra are normalized and shifted vertically for comparison. (b–d) Corresponding STM images of the surfaces after these preparations for coverage ≤1 ML (scan parameters: I_t = 1 pA, V = −0.15 V).

of adjacent DCPDMbpy ligands in a Fe(DCPDMbpy)$_2$ species that was constrained to a planar conformation on a surface.

XPS Study of the Complex on Au(111). To investigate the role of Fe adatoms in the assembly process, we further investigated by XPS the N1s binding energies (BE) of the DCPDMbpy molecules on Au(111) to reveal the chemical environment of the bpy moieties. The samples were prepared at RT with a coverage ≤1 ML in the preparation chamber of the LT microscope and then transferred using a UHV-vacuum suitcase to the XPS chamber for analysis (see Methods). For this specific coverage, the N 1s BE is at 398.2 eV (green curve in Figure 4a), which corresponds to supramolecular networks of the transoid molecules (Figure 4b). Upon complex formation obtained by additionally depositing Fe adatoms (blue curve in Figure 4a), the N 1s BE significantly shifts by 1 eV to higher values (BE = 399.2 eV) supporting the expected Fe complex formation and with this also the switch to cisoid conformation. In that case, the lone pair of the N atoms of the bpy preferentially interacts with an Fe adatom,[32,33] inducing a new chemical environment for the nitrogens (N···Fe···N). After annealing of the surface covered with DCPDM(bpy) molecules at 400 K (without Fe deposition), the N 1s BE shifts slightly by 0.2 eV. According to the STM image (Figure 4c), the shift originates from a fraction of DCPDMbpy molecules that have formed a complex with specific sites of the gold surface such as step edges, defects, and elbows of the reconstruction (black arrows in Figure 4c).[28] Although two peaks are expected here, the first arising from the transoid–DCPDMbpy molecules and the second from the Au–DCPDMbpy coordination complexes (N···Au···N), the small amount of molecules (<1 ML), for example low signal-to-noise ratio, do not allow a proper deconvolution of the N 1s peaks, and hence, only one peak is observed. Moreover, the complex formation reaction only triggered by temperature without additional metal atoms is less efficient as it is restricted to specific locations of the Au(111) surface.

Table 1 summarizes the DCPDMbpy conformation ratio as a function of the sample preparations at a coverage ≤0.1 ML

Table 1. Effect of Fe and Annealing on the DCPDMbpy Conformation for Less Than 0.1 ML Coverage

	without Fe without annealing	without Fe with annealing	with Fe with annealing
transoid	91%	52%	3%
cisoid	9%	48%	97%

adsorbed on Au(111). This ratio could be determined through analysis of a set of high resolution STM images. Upon deposition at RT, almost all the DCPDMbpy molecules adsorbed on the Au(111) surface are in transoid conformation and the ratio transoid/cisoid is measured to be ∼91:9. Upon Fe deposition and surface annealing, this ratio changes to 3:97, demonstrating a high specificity for the complex formation. When only triggered by temperature, the ratio becomes ∼52:48 but might be increased for higher molecule coverages as it will allow the saturation of the Au(111) reactive sites. It is also worth mentioning that metallic surfaces are known for their catalytic character in contrast to other surfaces. In a previous investigation, the study of the temperature effect on the DCPDMbpy assembly on NiO(001)[18] demonstrated that molecules are not affected by annealing and remain in transoid conformation up to 493 K when they tend to desorb. In principle, the process is thus independent of the underlying surface as soon as metal adatoms are present as demonstrated on both Au(111) and NiO(001) surfaces. As shown in our work, the diffusion and local reactive sites of the surfaces, however, influence the complex reaction and other metals might also form complexes. Finally, we emphasize the irreversible character of this prochiral to achiral transition in single molecules as well as in supramolecular networks because the opposite change, from cisoid to transoid, could not be experimentally achieved. Our results thus show the formation and suppression of surface-induced prochirality from the single molecule scale to the supramolecular network level.

CONCLUSIONS

In summary, the DCPDMbpy molecule is adsorbed in a transoid geometry on both NiO(001) and Au(111) as single molecules and enantiopure domains, respectively. When adsorbed on NiO(001) partially covered with Fe adatoms, the molecule shows a cisoid conformation demonstrating the formation of a metal-coordination complex (Fe–DCPDMbpy). On Au(111), we showed that the molecules undergo the interconversion from transoid to cisoid upon Fe adatom deposition on previously formed enantiopure DCPDMbpy assemblies. Using AFM imaging and XPS measurements, we demonstrated that the process is triggered by coordination complex formation between Fe atoms and the bpy moieties of the molecule. Interestingly, the new Fe–DCPDMbpy supramolecular networks on gold are achiral, which demonstrates the suppression of a surface-induced chirality in thin supramolecular networks via metal complex formation.

DOI: 10.1021/acsomega.8b01792
ACS Omega 2018, 3, 12851−12856

METHODS

Molecule Synthesis. DCPDMbpy was synthesized by Dr. Davood Zare (University of Basel) following the reported procedure.[34]

Sample Preparation. The NiO(001) crystals used in this study, purchased from SurfaceNet, consist of rectangular rods with dimensions $2 \times 2 \times 7$ mm^3 and a long axis in the [001] direction. The NiO(001) surface was prepared through in situ cleavage (UHV, $p < 1 \times 10^{-10}$ mbar) with prior and subsequent annealing at about 800 K resulting in an atomically clean surface. An Au(111) single crystal, purchased from Mateck GmbH, was cleaned by several sputtering and annealing cycles in UHV conditions. DCPDMbpy molecules were thermally evaporated from a Knudsen cell heated up to 528 K on the surfaces kept at RT. The molecule rate was checked in situ using a quartz microbalance. Fe adatom depositions were conducted using an e-beam evaporator. To promote complex formation, the sample was then annealed to 420 K during molecule and atom evaporation. For NiO(001), because of the low diffusion rate, we first sublimated the Fe atoms and then DCPDMbpy molecules. For Au(111), the steps of the procedure were inverted: molecules were deposited first and Fe atoms afterward. A vacuum suitcase from Ferrovac GmbH was employed to transfer samples from the UHV LT AFM/STM setup to the XPS chamber.

AFM Imaging at RT. AFM measurements on NiO were conducted with a home built AFM system in UHV operated at RT. All AFM images were recorded in the non-contact mode (nc-AFM), using a silicon cantilever (Nanosensors PPP-NCR stiffness k = 20−30 N/m, resonance frequency f_1 around 165 kHz, and Q_1 factor around 30 000 with compensated contact potential difference).

STM/AFM Imaging at Low Temperature. STM/AFM experiments were carried out at 4.7 K with an Omicron GmbH low-temperature STM/AFM system operated with a Nanonis RC5 electronics. We used commercial tuning fork sensors in the qPlus configuration (f_1 = 26 kHz, Q = 10 000−25 000, nominal spring constant k = 1800 N m^{-1}). The constant-height AFM images were acquired with CO-terminated tips. All voltages refer to the sample bias with respect to the tip.

XPS Measurements. The samples were transferred in situ using a vacuum suitcase to the XPS chamber directly after molecules and Fe atom deposition. The pressure in the XPS chamber was always $\leq 10^{-10}$ mbar, and measurements were performed using a VG ESCALAB 210 system equipped with a monochromatic Al K_α radiation source. A pass energy of 20 eV was used for all narrow scan measurements and 100 eV pass energy for survey scans. Normal electron escape angle and a step size of 0.05 eV were used. The energy positions of the spectra were calibrated with reference to the 4f 7/2 level of a clean gold sample at 84.0 eV binding energy. XPS fitting was performed with Unifit 2016 Software.[35]

AUTHOR INFORMATION

Corresponding Author

*E-mail: remy.pawlak@unibas.ch.

ORCID

Rémy Pawlak: 0000-0001-8295-7241
Antoine Hinaut: 0000-0002-2608-2564
Catherine E. Housecroft: 0000-0002-8074-0089

Author Contributions

S.F., A.H., C.E.H., and T.G. conceived the experiment. S.F. measured the RT-AFM on NiO. R.P. measured with the LT-STM/AFM on Au(111). L.M. and R.S. performed the XPS measurements. S.F. wrote the manuscript with the help of R.P. All co-authors contributed to project concepts and discussion and read and commented on the manuscript.

Notes

The authors declare no competing financial interest.

ACKNOWLEDGMENTS

This work was supported by the Swiss National Science Foundation (SNF) CR22I2-156236, the Swiss Nanoscience Institute (SNI), and the University of Basel.

REFERENCES

(1) Moss, G. P. Basic terminology of stereochemistry. *Pure and App. Chemistry* **1996**, *68*, 2193. Muller, P. Glossary of terms used in physical organic chemistry. *Pure and App. Chemistry* **1994**, *66*, 1112.

(2) Raval, R. Chiral Expression From Molecular Assemblies at Metal Surfaces: Insights From Surface Science Techniques. *Chem. Soc. Rev.* **2009**, *38*, 707−721.

(3) Ernst, K.-H. Molecular chirality at surfaces. *Phys. Status Solidi B* **2012**, *249*, 2057−2088.

(4) Stetsovych, O.; Švec, M.; Vacek, J.; Chocholoušová, J. V.; Jančařík, A.; Rybáček, J.; Kosmider, K.; Stará, I. G.; Jelínek, P.; Starý, I. From helical to planar chirality by on-surface chemistry. *Nat. Chem.* **2017**, *9*, 213−218.

(5) Wäckerlin, C.; Li, J.; Mairena, A.; Martin, K.; Avarvari, N.; Ernst, K.-H. Surface-assisted diastereoselective Ullmann coupling of bishelicenes. *Chem. Commun.* **2016**, *52*, 12694−12697.

(6) Verbiest, T.; Van Elshocht, S.; Kauranen, M.; Hellemans, L.; Snauwaert, J.; Nuckolls, C.; Katz, T. J.; Persoons, A. Strong Enhancement of Nonlinear Optical Properties Through Supramolecular Chirality. *Science* **1998**, *282*, 913−915.

(7) Rosenberg, R. A.; Haija, M. A.; Ryan, P. J. Chiral-Selective Chemistry induced by spin-polarized secondary electrons from a magnetic substrate. *Phys. Rev. Lett.* **2008**, *101*, 178301.

(8) Ray, K.; Ananthavel, S. P.; Waldeck, D. H.; Naaman, R. Asymmetric scattering of polarized electrons by organized organic films of chiral molecules. *Science* **1999**, *283*, 814−816.

(9) Kottas, G. S.; Clarke, L. I.; Horinek, D.; Michl, J. Artificial molecular rotors. *Chem. Rev.* **2005**, *105*, 1281−1376.

(10) Browne, W. R.; Feringa, B. L. Making molecular machines work. *Nat. Nanotechnol.* **2006**, *1*, 25−35.

(11) McCarthy, M.; Guiry, P. J. Axially chiral bidentate ligands in asymmetric catalysis. *Tetrahedron* **2001**, *57*, 3809−3844.

(12) Ohtani, B.; Shintani, A.; Uosaki, K. Two-Dimensional Chirality: Self-Assembled Monolayer of an Atropisomeric Compound Covalently Bound to a Gold Surface. *J. Am. Chem. Soc.* **1999**, *121*, 6515−6516.

(13) Hinaut, A.; Meier, T.; Pawlak, R.; Feund, S.; Jöhr, R.; Kawai, S.; Glatzel, T.; Decurtins, S.; Müllen, K.; Narita, A.; Liu, S.-X.; Meyer, E. Electrospray deposition of structurally complex molecules revealed by atomic force microscopy. *Nanoscale* **2018**, *10*, 1337−1344.

(14) Malzner, F.; Housecroft, C.; Constable, E. The versatile SALSAC approach to heteroleptic copper(I) dye assembly in dye-sensitized solar cells. *Inorganics* **2018**, *6*, 57.

(15) Schönhofer, E.; Bozic-Weber, B.; Martin, C. J.; Constable, E. C.; Housecroft, C. E.; Zampese, J. A. 'Surfaces-as-ligands, surfaces-as-complexes' strategies for copper(I) dye-sensitized solar cells. *Dyes and Pigments* **2015**, *115*, 154−165.

(16) Bozic-Weber, B.; Constable, E. C.; Housecroft, C. E.; Kopecky, P.; Neuburger, M.; Zampese, J. A. The intramolecular aryl embrace: from light emission to light absorption. *Dalton Trans.* **2011**, *40*, 12584−12594.

DOI: 10.1021/acsomega.8b01792
ACS Omega 2018, 3, 12851−12856

(17) Malzner, F. J.; Prescimone, A.; Constable, E. C.; Housecroft, C. E.; Willgert, M. Exploring simple ancillary ligands in copper-based dye-sensitized solar cells: effects of a heteroatom switch and of co-sensitization. *J. Mater. Chem. A* **2017**, *5*, 4671−4685 and references therein .
(18) Freund, S.; Hinaut, A.; Marinakis, N.; Constable, E. C.; Meyer, E.; Housecroft, C. E.; Glatzel, T. Anchoring of a dye precursor on NiO(001) studied by non-contact atomic force microscopy. *Beilstein J. Nanotechnol.* **2018**, *9*, 242−249.
(19) Göller, A.; Grummt, U.-W. Torsional barriers in biphenyl, 2,2'-bipyridine and 2-phenylpyridine. *Chem. Phys. Lett.* **2000**, *321*, 399−405.
(20) Howard, S. T. Conformers, Energetics, and Basicity of 2,2'-Bipyridine. *J. Am. Chem. Soc.* **1996**, *118*, 10269−10274.
(21) Sanfeliciano, S. M. G.; Schaus, J. M. Rapid assessment of conformational preferences in biaryl and aryl carbonyl fragments. *PloS One* **2018**, *13*, No. e0192974.
(22) Amabilino, D. B.; Tait, S. L. Complex molecular surfaces and interfaces: concluding remarks. *Faraday Discuss.* **2017**, *204*, 487−502.
(23) Rodgers, M. T.; Stanley, J. R.; Amunugama, R. Periodic trends in the binding of metal ions to pyridine studied by threshold collision-induced dissociation and density functional theory. *J. Am. Chem. Soc.* **2000**, *122*, 10969−10978.
(24) Moreno, C.; Stetsovych, O.; Shimizu, T. K.; Custance, O. imaging three-dimensional surface objects with submolecular resolution by atomic force microscopy. *Nano Lett.* **2015**, *15*, 2257−2262.
(25) Iwata, K.; Yamazaki, S.; Mutombo, P.; Hapala, P.; Ondráček, M.; Jelinek, P.; Sugimoto, Y. Chemical structure imaging of a single molecule by atomic force microscopy at room temperature. *Nat. Commun.* **2015**, *6*, 7766.
(26) Kawai, S.; Sadeghi, A.; Okamoto, T.; Mitsui, C.; Pawlak, R.; Meier, T.; Takeya, J.; Goedecker, S.; Meyer, E. Organometallic bonding in an Ullmann-Type on-surface chemical reaction studied by high-resolution atomic force microscopy. *Small* **2016**, *12*, 5303−5311.
(27) Kocić, N.; Liu, X.; Chen, S.; Decurtins, S.; Krejčí, O.; Jelínek, P.; Repp, J.; Liu, S.-X. Control of reactivity and regioselectivity for on-surface dehydrogenative aryl-aryl bond formation. *J. Am. Chem. Soc.* **2016**, *138*, 5585−5593.
(28) Pawlak, R.; Meier, T.; Renaud, N.; Kisiel, M.; Hinaut, A.; Glatzel, T.; Sordes, D.; Durand, C.; Soe, W.-H.; Baratoff, A.; Joachim, C.; Housecroft, C. E.; Constable, E. C.; Meyer, E. Design and characterization of an electrically powered single molecule on gold. *ACS Nano* **2017**, *11*, 9930−9940.
(29) Zint, S.; Ebeling, D.; Schlöder, T.; Ahles, S.; Mollenhauer, D.; Wegner, H. A.; Schirmeisen, A. Imaging successive intermediate states of the on-surface Ullmann reaction on Cu(111): role of the metal coordination. *ACS Nano* **2017**, *11*, 4183−4190.
(30) Krull, C.; Castelli, M.; Hapala, P.; Kumar, D.; Jelinek, P.; Schiffrin, A. Iron-based trinuclear metal-organic nanostructures on a surface with local charge accumulation. *Nat. Commun.* **2018**, *9*, 3211.
(31) Gross, L.; Mohn, F.; Liljeroth, P.; Repp, J.; Giessibl, F. J.; Meyer, G. Measuring the Charge State of an Adatom with Noncontact Atomic Force Microscopy. *Science* **2009**, *324*, 1428−1431.
(32) Shchyrba, A.; Nguyen, M.-T.; Wäckerlin, C.; Martens, S.; Nowakowska, S.; Ivas, T.; Roose, J.; Nijs, T.; Boz, S.; Schär, M.; Stöhr, M.; Pignedoli, C. A.; Thilgen, C.; Diederich, F.; Passerone, D.; Jung, T. A. Chirality transfer in 1D self-assemblies: influence of H-bonding vs metal coordination between dicyano[7]helicene enantiomers. *J. Am. Chem. Soc.* **2013**, *135*, 15270−15273.
(33) Meier, T.; Pawlak, R.; Kawai, S.; Geng, Y.; Liu, X.; Decurtins, S.; Hapala, P.; Baratoff, A.; Liu, S.-X.; Jelínek, P.; Meyer, E.; Glatzel, T. Donor-acceptor properties of a single-molecule altered by on-surface complex formation. *ACS Nano* **2017**, *11*, 8413−8420.
(34) Hernández Redondo, A. Copper(I) polypyridine complexes: the sensitizers of the future for dye-sensitized solar cells (DSSCs), Ph.D. Thesis, University of Basel, 2009.
(35) Hesse, R.; Chassé, T.; Szargan, R. Peak shape analysis of core level photoelectron spectra using UNIFIT for WINDOWS. *Fresenius. J. Anal. Chem.* **1999**, *365*, 48−54.

DOI: 10.1021/acsomega.8b01792
ACS Omega 2018, 3, 12851−12856